Title

Genomic characterization of a three-dimensional skin model following exposure to ionizing radiation

Permalink

https://escholarship.org/uc/item/7kb8z3ht

Journal

Journal of Radiation Research, 53(6)

ISSN

1040-9564

Authors

Yunis, Reem
Albrecht, Huguette
Kalanetra, Karen M
et al.

Publication Date

2012-11-01

DOI

10.1093/jrr/rrs063

Peer reviewed

Genomic characterization of a three-dimensional skin model following exposure to ionizing radiation

Reem YUNIS, Huguette ALBRECHT*, Karen M. KALANETRA,
Shiquan WU and David M. ROCKE

Department of Public Health Sciences, University of California at Davis School of Medicine, One Shields Avenue, Davis,
CA 95616, USA
*Corresponding author: Tel: +1-916-734-7421; Fax: +1-916-457-4306; Email: huguette.albrecht@ucdmc.ucdavis.edu

This study aimed at characterizing the genomic response to low versus moderate doses of ionizing radiation (LDIR versus MDIR) in a three-dimensional (3D) skin model, which exhibits a closer tissue complexity to human skin than monolayer cell cultures. EpiDermFT skin plugs were exposed to 0, 0.1 and 1 Gy doses of X-rays and harvested at 5 min, 3, 8 and 24 h post-irradiation (post-IR). RNA was interrogated for global gene expression alteration. Our results show that MDIR modulated a larger number of genes over the course of 24 h compared to LDIR. However, immediately and throughout the first 3h post-IR, LDIR modulated a larger number of genes than MDIR, mostly associated with cell–cell signaling and survival promotion. Significant modulation of pathways was detected only at 3 h post-IR in MDIR with induction of genes promoting apoptosis. Collectively, the data show different dynamics in the response to LDIR versus MDIR, especially in cell-cycle distribution. LDIR-exposed tissues showed signs of attempted cell-cycle re-entry as early as 3 h post-IR, but were arrested beyond 8 h at the G1/S checkpoint. At 24 h, cells appeared to accumulate at the G2/M checkpoint. MDIR-exposed tissues did not exhibit a prolonged G1/S arrest but rather a prolonged G2/M arrest, which was sustained at least up to 24 h. By 24 h cells exhibited signs of recovery in both LDIR- and MDIR-exposed tissues. In summary, the most pronounced difference in the initial cellular response to LDIR versus MDIR is the promotion of protection and survival in LDIR versus the promotion of apoptosis in MDIR.

Keywords: low dose ionizing radiation; EpiDermFT; gene expression; microarray

INTRODUCTION

The human body is constantly exposed to radiation, through occupational exposure, environmental exposure, or through medical diagnostics or therapy. Except for radiotherapy in the target area, these exposures generally involve low doses (≤0.1 Gy) compared to moderate (1–10 Gy) and high doses (>10 Gy) used in therapy, or as a result of accidental irradiation.

The biological effects and assessment of health risk in humans following exposure to low-dose ionizing radiation (LDIR) are ambiguous and have been the central stage for intense debate among radiobiologists [1–4]. Thus far, and supported by the Biological Effects of Ionizing Radiation [5], carcinogenic risks following exposure to LDIR are extrapolated from the linear no-threshold (LNT) model that assumes a linear relationship between dose and effect [3, 6]. However, a plethora of studies are showing evidence for other effects of LDIR such as hyper-radiosensitivity, the bystander effect, and adaptive response [7], stressing the importance of elucidating its effects on human health, especially with the increasing frequency of diagnostic radiology and body scan exposures.

Cellular and molecular responses to moderate and high IR doses are well established, but, in the range of low dose, these responses are still poorly defined. The widely accepted paradigm is that ionizing radiation causes direct and indirect DNA damage in cells, and consequently triggers the DNA damage response (DDR) pathway. This pathway is a well-concerted cascade of signal transduction, which includes sensors that detect DNA damage, transducers that produce signals, and effectors that induce cell

cycle arrest and death [8]. Alteration of gene expression is a significant component of the response to IR, and with advances in genomic technologies and data-mining, global gene expression profiling is now considered a standard approach in obtaining information about cellular responses to radiation. However, no consensus has been achieved regarding the genomic response to radiation due to the variability of experimental models that include cell and tissue types, doses, dose rates, post-exposure times and data processing. Notably, when addressing the question of whether LDIR has similar or different effects on gene expression to higher radiation doses, it is important to carry out such studies side by side to minimize experimental variation that may have an impact on gene expression.

Skin makes up the largest organ of the body and is likely to be the first to encounter radiation, thus reinforcing the importance of elucidating the cellular and molecular responses in skin. The limited accessibility to human tissue necessitates the pursuit of reliable *in vitro* models. Monolayer cell cultures are the system of choice in laboratories, and are widely used in studying molecular and cellular processes. However cell monocultures neither reproduce a 3D environment nor interactions between different cell types. The dampened radiosensitivity observed between 2D and 3D grown cells [9] appears to be linked to a difference in chromatin condensation; in 3D grown cells increased levels of heterochromatin confer radioresistance [10].

EpiDermFT™ (MatTek Corporation) is a 3D full thickness skin model that is composed of normal human epidermal keratinocytes (NHEK) and normal human dermal fibroblasts (NHDF), which reproduces a complex tissue environment [11]. This model is widely used instead of animals for assessing toxicity of cosmetics and topical agents in human skin. In recent years EpiDermFT has been used in other fields of investigation such as carcinogenesis [12–14], and wound healing [11]. EpiDermFT has also become an attractive *in vitro* model for radiation studies in the skin [15–20]. Using this 3D skin model, Belyakov *et al.* [21] showed the existence of the bystander effect, a phenomenon that was initially found and described in single-cell monolayer cultures. This study suggested the importance of using models that better reproduce the complexity of human tissues to study the relevance of biological observations. The reported persistence for 6–7 days of high numbers of DNA double-strand breaks in EpiDermFT compared to only 3 days in monolayer cultures [22], suggests that a series of more complex cell signaling events occur in EpiDermFT, thereby emphasizing the contribution of the microenvironment in shaping the cellular response.

In the present study, we sought to characterize the genomic alterations in the EpiDermFT human skin model following 0.1 Gy and 1 Gy doses of X-ray ionizing radiation over a 24 h time period.

MATERIALS AND METHODS

Tissue
The EpiDermFT-400 *in vitro* skin tissue model is a reconstructed, normal human 3D full thickness model that is generated by growing NHEK on NHDF, reproducing the epidermis and dermis layers of normal skin (MatTek Corporation, Ashland, MA). The tissues are cultured in 6-well plates using an air–liquid interface technique that promotes cell differentiation [21–23]. The engineered tissue exhibits *in vivo*-like growth and morphological characteristics, and the cells sustain differentiation and metabolic status similar to those of human epidermis [24]. As per the manufacturer's recommendations, upon arrival, 24 plugs were immediately transferred to 6-well plates with 2 ml EFT-400 medium and incubated overnight at 37°C, under 5% CO_2 atmospheric conditions. After overnight equilibration, the medium was replaced with a pre-warmed fresh supply. Plates were sealed and transferred under ambient conditions to the clinical irradiator at the Department of Radiation Oncology of the UC Davis Medical Center.

Irradiation
Tissues were irradiated using the Elekta Synergy clinical irradiator (Stockholm, Sweden) with 0, 0.1, and 1 Gy at a dose rate of 0.5 Gy/min. Skin plugs were harvested at 5 min, 3, 8 and 24 h post-IR. The designated 5 min timepoint tissues were collected and stored in RNAlater (Qiagen, Valencia, CA) at the clinic under ambient conditions. The remaining tissue plugs were returned to the laboratory and kept at 37°C/5% CO_2 conditions for the length of the incubation time before being harvested and stored in RNAlater. Tissue plugs were cut in half and stored in 2 ml RNAlater at 4°C for 3 days, after which they were transferred to –20°C till RNA extraction.

Total RNA extraction and processing for microarray analysis
Each tissue plug was transferred to 1 mL Buffer RLT (Qiagen) in Lysing Matrix D tubes (Qbiogene, Irvine, CA) and subjected to physical disruption in a Fastprep Beat Beater (Qbiogene). Complete lysis of the tissue was obtained after 5 rounds of bead beating (5 m/s for 40 seconds each round). Between disruption rounds, tubes were placed on ice for one minute. After lysis, samples were centrifuged at 14 000 × *g* for 5 min at room temperature. Supernatant was subjected to total RNA extraction using RNeasy kit (Qiagen) as per manufacturer's instructions. RNA integrity was verified using Agilent 2100 Bioanalyzer (Santa Clara, CA), and 300 ng total RNA was reverse transcribed, amplified and labeled using the Illumina TotalPrep RNA amplification kit (Ambion, Austin, TX). Resulting cRNAs were hybridized to Illumina

HumanRef-8 expression beadchips (version 3; Illumina, Hayward, CA) and interrogated at the UC Davis Expression Analysis Core.

Gene expression analysis

Each beadchip contained 8 microarrays, thus 3 beadchips were used to analyze 24 samples. The steps used for data processing and analysis were as follows:

(i) The microarray data were processed by BeadStudio 3.4.0 using the HumanRef-8-V3-R0 settings with background subtraction, but no normalization. Each array contains values for 24 526 RefSeq curated gene probes and 11 control probes (www.switchtoi.com/resources). We analyzed each probe separately rather than combining the data from multiple probes corresponding to the same gene.

(ii) Two BioConductor packages lumi 1.2.0 and arrayQualityMetrics 2.2.3 were used to detect outliers. Density plots, MA-plots, Boxplots, and Heatmaps/clustering for samples showed no outlying samples or other quality problems.

(iii) Using BeadStudio probes with detection, P-values > 0.05 across all samples were filtered out, resulting in a final set of 15 964 probes.

(iv) Transformation and normalization of the data was performed to stabilize the variance and to eliminate systematic array bias. The LMGene 2.0 R package was used to estimate the parameters of the glog transformation, followed by quantile analysis [25–29].

Pathway analysis

The list of significant probes for each dose comparison within each time-point was uploaded onto the server-based software, MetaCore™ by GENEGO® (version 6.2, build 24095; http://www.genego.com/). This analysis software maps differentially-expressed genes to canonical pathway maps and networks. It is based on a proprietary manually-curated database of human protein-protein, protein-DNA and protein compound interactions, metabolic and signaling pathways. MetaCore provides over 2000 canonical signaling and metabolism pathway analysis maps. The P-values throughout MetaCore are derived essentially from Fisher's exact test for the number of genes in the pathway or gene group that are significant compared to the number outside the pathway or gene group that are significant. These are given as raw P-values and also as false discovery rate (FDR)-adjusted P-values over the set of pathways and gene groups that have been analyzed.

RESULTS

Statistical analysis

For each probe or gene (since the majority of genes was detected by a single probe) we have three doses (0, 0.1, and 1 Gy) and four time points (5 min, 3 h, 8 h, and 24 h). We began with a two-way ANOVA for each probe with the main effects of dose and time and the interaction effect. Lists of genes responsive to radiation were generated by selecting those showing significant main effect of dose and/ or dose-by-time interaction at 10% False Discovery Rate (FDR) [30]. There were 8924 genes exhibiting a significant response to dose and/or dose-by-time complex effects. Since the majority of complex effects accompany a significant time effect, and since time effects *in vitro* are not themselves of interest, pathway analyses were focused only on genes exhibiting dose effects; there were 5753 of these significant at the 10% FDR. For this subset, and for each time of at least one hour and non-zero dose, we compared the mean response at that dose and time to the mean response for that dose at the earliest time (5 min) in order to identify genes whose expression is changed by that dose of radiation at that time. We used the ANOVA RMSE for the denominator for these tests in order to have sufficient statistical power. If the P-value of the t-test was less than 0.05, we considered this as statistically significant, without further accounting for multiple comparisons, since only genes were used where the dose effect was significant at an FDR of 10%. Consequently, two gene lists, one for each IR dose tested, were generated for each post-IR time analyzed. Gene lists were subjected to pathway analysis using a 5% FDR.

Gene expression 5 min post-IR

Radiation induced almost instant changes in gene expression in EpiDermFT as deduced from comparison with the non-irradiated tissues that were handled similarly.

In the 0.1 Gy-irradiated group, 752 genes were differentially expressed, of which 408 were upregulated and 344 were downregulated (Fig. 1). A smaller set of genes, 490, was modulated in the 1 Gy-irradiated group with 272 and 218 up- and downregulated, respectively.

The genes that were modulated after 1 Gy exposure were mainly associated with DNA damage and apoptosis (Table 1), whereas genes that were modulated after 0.1 Gy exposure were associated with a wide range of cellular processes (DNA damage, apoptosis, inflammatory response and cell differentiation), represented in 48 significant pathways (Tables 2 and 3). The initial response of EpiDermFT cells to 0.1 Gy appeared to be blockage of apoptosis and promotion of survival, exhibited by the induction of the survival transcription factors NF-κB and c-Jun (upregulation of NF-κB2, RELB, JUN) (Table 1). In addition, the NF-κB pathway intersected with the apoptotic pathway via
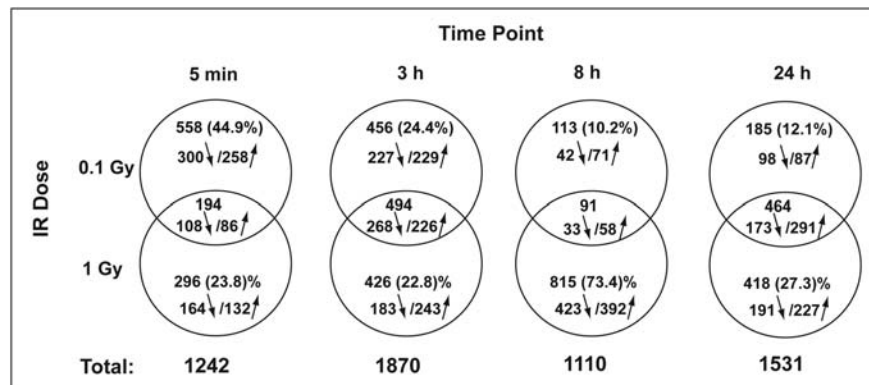
Fig. 1. Venn diagram illustrating the numbers of significantly differentially expressed genes. Percentage and number of up- and downregulated genes in EpidermFT after 0.1 or 1 Gy exposure over a course of 24 h post-IR.

upregulation of the gene encoding the cellular inhibitor of apoptosis c-IAP2, which inhibits the activity of several caspases by directly binding to them. There was also upregulation of TNFR2 (tumor necrosis factor receptor), which promotes survival via the NF-κB pathway, and downregulation of TNFR1, which promotes apoptosis via caspase activation.

Genes modulated by only one dose at a given time-point were defined as exclusive genes for that dose–time combination. At 5 min post-IR, ~45% of 1242 radiation-responsive genes were exclusive to 0.1 Gy, compared to only ~24% to 1 Gy (Fig. 1). A substantial subset of the 0.1 Gy-exclusive genes was associated with inflammatory and survival responses. Genes exclusive to 0.1 Gy were associated with the DDR pathway (data not shown), but were not enough to result in any significant pathway placement.

Gene expression 3 h post-IR
Three hours post-IR showed the highest number of radiation-responsive genes, totaling 1870, with similar numbers of genes exclusively modulated by each dose that were divided similarly between up- and downregulation (Fig. 1). Responses to 0.1 and 1 Gy significantly involved 8 and 2 cell-cycle regulation pathways, respectively (Table 2). Modulation of the ESR1 (estrogen receptor 1) pathway was observed at both doses (Table 3), and resulted in cell cycle arrest at the G1/S checkpoint, supported by the upregulation of major cell cycle blockers such as p21, Rb, and p130 (Table 1). The SCF (S-phase kinase protein 1/Cullin/F-box) complex, an E3-ubiquitin ligase that targets p21 and p130 for degradation, was inactivated, as suggested by the downregulation of genes encoding proteins with key roles in this pathway (PLK1, CDC25A and F-box subunits [CKS1, SKP2, and FBXW7]) (Table 1). APC (anaphase promoting complex), which was modulated by 0.1 Gy only, is another ubiquitin ligase that mediates the degradation of SKP2 and CKS1, leading to the maintenance of G1 phase

and blockage from entry into S phase. Seven prosurvival pathways were significant at 0.1 Gy (Tables 2 and 3) involving the upregulation of NF-κB transfectors (RELA, RELB, NFKB2) and c-IAP2.

Tissues exposed to 1 Gy modulated nine proapoptosis pathways, as demonstrated by the upregulation of the proapoptotic TNFR superfamily members FasR (CD95) and DR5 (TNFRSF10B), and the upregulation of genes encoding GADD45α, NOXA, Bid, Bim, N-myristoyltransferase, and caspase-9 (Table 1). Moreover, SUMO-1 (which has inhibitory effects on FasR), PARP-1/-2 (which has a role in DNA damage repair), histone deacetylase class I (RBBP7) (that directly inhibits TP53 by deacetylation), and NADE encoding BEX3 protein (which has a role in cell growth), were all downregulated (Table 1).

About 24 and 23% of the genes modulated at 3 h post-IR were exclusive to 0.1 or 1 Gy, respectively (Fig. 1). Although these genes did not overlap, a subset of them was involved in similar cellular processes such as DNA damage, cell cycle regulation and apoptosis. The remaining subsets represented dose-exclusive processes such as an inflammatory response, cell differentiation, transcription regulation in response to 0.1 Gy, tissue remodeling and protein degradation in response to 1 Gy.

Gene expression 8 h post-IR
The number of genes with altered expression after 1 Gy irradiation was more than four times that altered by 0.1 Gy (906 vs 204, respectively; Fig. 1). Genes modulated by 1 Gy and 0.1 Gy affected 45 and 21 pathways, respectively (Table 2). Cell cycle regulation pathways were predominantly modulated by exposure to 1 Gy (13 pathways), compared to 0.1 Gy (only 6 pathways) (Table 2). Pathways shared between doses included DNA damage that was primarily mediated by ATM/ATR and BRCA1/BRCA2 (breast cancer-1/-2) pathways (Table 3). Modulation of these pathways reflected a suppression of DNA damage

Table 1. Functional pathways represented by significant differentially expressed genes

Time post-irradiation		5 min		3 h		8 h		24 h	
	Dose (Gy)	0.1	1	0.1	1	0.1	1	0.1	1
Gene name	Protein name				*P*-values				
ANLN	Anillin	_ [a]	–	*0.052* ↓ [b]	0.028 ↓	*0.069* ↓	0.015 ↓	0.003 ↓	<0.001 ↓
AURKA	Aurora A	–	–	–	–	–	–	0.033 ↓	0.005 ↓
AURKB	Aurora B	–	–	–	–	–	0.007 ↓	0.028 ↓	0.003 ↓
BARD1	Bard1	–	–	0.021 ↓	–	0.011 ↓	<0.001 ↓	–	<0.001 ↓
BCL2L11	Bim	–	–	–	0.020 ↑	–	*0.057* ↑	–	–
BID	Bid	0.010 ↑	–	0.002 ↑	0.004 ↑	–	–	*0.091* ↑	0.044 ↑
BIRC3	c-IAP2	0.009 ↑	–	0.007 ↑	–	–	–	–	0.050 ↑
BIRC5	Survivin	–	–	0.034 ↓	–	–	0.012 ↓	–	0.045 ↓
BRCA1	Brca1	–	–	–	–	0.006 ↓	<0.001 ↓	–	–
CASP1	Caspase-1	0.008 ↓	–	–	–	–	–	0.008 ↓	0.003 ↓
CASP6	Caspase-6	–	0.043 ↑	0.038 ↓	–	–	–	0.002 ↓	0.004 ↓
CASP9	Caspase-9	–	–	–	0.028 ↑	0.048 ↑	<0.001 ↑	*0.072* ↑	<0.001 ↑
CCNA2	Cyclin A	–	–	–	–	–	0.013 ↓	0.048 ↓	0.013 ↓
CCNB1	Cyclin B1	–	–	0.025 ↓	–	–	0.037 ↓	0.010 ↓	0.006 ↓
CCNB2	Cyclin B2	–	–	–	–	–	0.022 ↓	0.014 ↓	0.004 ↓
CDC2	CDK1 (p34)	–	–	0.024 ↓	–	*0.084* ↓	0.008 ↓	0.004 ↓	0.004 ↓
CDC7	CDC7	–	–	–	0.008 ↓	–	0.005 ↓	–	*0.063* ↓
CDC20	CDC20	–	–	–	–	–	0.027 ↓	–	–
CDC25A	CDC25A	–	–	–	0.036 ↓	0.016 ↓	<0.001 ↓	–	–
CDC25B	CDC25B	*0.089* ↓	–	–	–	–	0.003 ↓	0.029 ↓	*0.062* ↓
CDC25C	CDC25C	–	–	–	–	–	–	0.001 ↓	<0.001 ↓
CDK2	CDK2	–	–	0.017 ↑	–	–	0.008 ↑	–	*0.060* ↑
CDK6	CDK6	<0.001 ↑	–	0.047 ↑	–	–	–	–	0.008 ↑
CDKN1A	p21	*0.053* ↑	–	0.015 ↑	<0.001 ↑	0.025 ↑	<0.001 ↑	–	0.008 ↑
CDT1	Cdt1	–	–	–	–	–	0.006 ↓	–	–
CKS1B	CKS1	–	–	0.029 ↓	–	–	0.006 ↓	–	–
DRAM	DRAM	0.002 ↑	–	*0.063* ↑	0.033 ↑	–	<0.001 ↑	–	0.016 ↑
FANCD2	FANCD2	–	–	–	–	–	0.012 ↓	–	–
FAS	FasR (CD95)	–	–	–	0.009 ↑	–	*0.060* ↑	–	–
FBXW7	F-box W7	–	–	*0.058* ↓	0.012 ↓	*0.099* ↓	–	0.003 ↓	0.020 ↓
FOS	c-Fos	0.004 ↓	–	*0.097* ↑	<0.001 ↑	–	0.048 ↑	0.038 ↓	0.024 ↓
GADD45A	GADD45α	–	*0.053* ↑	–	0.006 ↑	–	–	*0.078* ↓	–
HSPA2	HSP70 prtn2	0.006 ↓	–	0.002 ↓	–	–	–	<0.001 ↓	<0.001 ↓
IL6	IL-6	0.011 ↑	–	0.010 ↑	0.011 ↑	–	0.023 ↑	–	*0.099* ↑
IRAK2	IRAK2	0.021 ↑	–	0.036 ↑	–	–	–	0.023 ↑	0.002 ↑
IRAK3	IRAK3	0.006 ↑	–	0.036 ↑	–	–	0.040 ↑	*0.083* ↑	0.023 ↑
JUN	c-Jun	<0.001 ↑	–	0.015 ↑	0.004 ↑	–	0.022 ↑	–	*0.094* ↑

Continued

Table 1. *Continued*

Time post-irradiation		5 min		3 h		8 h		24 h	
	Dose (Gy)	0.1	1	0.1	1	0.1	1	0.1	1
KIF11	KNSL1	–	–	–	0.048 ↓	–	0.022 ↓	0.003 ↓	0.002 ↓
LIG3	DNA ligase III	–	0.016 ↓	–	–	–	–	0.011 ↑	0.037 ↑
LMNB1	Lamin B1	–	–	–	–	–	0.009 ↓	–	–
MAP3K4	MEKK4	–	–	*0.066* ↑	–	–	0.026 ↑	–	0.021 ↑
MAPK10	JNK	–	0.021 ↑	0.030 ↑	0.037 ↑	–	0.030 ↑	*0.079* ↑	0.015 ↑
MCM (2-7)	MCM complex	–	–	–	–	–	<0.001 ↓	–	–
MCM10	MCM complex	–	–	–	0.037 ↓	0.017 ↓	<0.001 ↓	–	0.032 ↓
MDM2	MDM2	–	–	–	0.029 ↑	–	0.003 ↑	–	–
MDM4	MDM4	–	0.007 ↑	–	–	–	0.043 ↑	–	–
MMP1	MMP-1	0.014 ↑	–	*0.082* ↑	–	–	–	–	–
MMP2	MMP-2	0.038 ↑	–	0.004 ↑	–	–	0.017 ↑	–	0.033 ↑
MYL9	MYRL2	0.015 ↓	–	0.002 ↓	0.002 ↓	0.004 ↓	*0.052* ↓	0.010 ↓	0.017 ↓
NADE	BEX3	0.019 ↓	*0.088* ↓	0.048 ↓	0.017 ↓	*0.084* ↓	0.027 ↓	0.021 ↓	–
NCAPG	CAP-G	–	–	*0.088* ↓	–	*0.093* ↓	0.003 ↓	0.035 ↓	0.003 ↓
NFKB2	NF-κB (p52)	0.022 ↑	–	0.033 ↑	0.016 ↑	–	–	–	–
NMT1	N-myristoyl-transferase	–	–	*0.057* ↑	0.038 ↑	–	–	–	0.029 ↑
NUMA1	NUMA-1	–	–	–	–	–	0.017 ↓	–	–
ORC1L	ORC1L	–	–	–	0.042 ↓	–	<0.001 ↓	–	0.033 ↓
PARP1	PARP-1	–	–	–	0.042 ↓	*0.059* ↓	0.005 ↓	0.004 ↓	0.008 ↓
PARP2	PARP-2	*0.059* ↓	–	0.003 ↓	0.001 ↓	*0.081* ↓	<0.001 ↓	*0.094* ↓	0.011 ↓
PCNA	PCNA	–	–	0.012 ↓	–	0.037 ↓	–	0.039 ↓	*0.068* ↓
PLK1	PLK1	–	–	–	0.004 ↓	–	–	–	<0.001 ↓
PLK4	PLK4	–	–	–	–	–	0.006 ↓	–	0.035 ↓
PMAIP1	NOXA	–	–	–	0.001 ↑	–	–	–	–
POLD1	POL delta cat (p125)	–	0.002 ↓	0.024 ↓	–	–	0.002 ↓	–	–
POLE2	POL epsilon 2(p59)	–	–	–	0.049 ↓	–	0.003 ↓	–	–
PTGS2	COX-2	0.029 ↑	–	0.002 ↑	0.003 ↑	–	0.034 ↑	–	*0.084* ↑
PTTG1	Securin	–	–	–	–	–	–	0.022 ↓	0.032 ↓
RAD1	RAD1	0.019 ↓	–	0.007 ↓	0.002 ↓	–	–	–	–
RAD23B	RAD23B	–	–	0.027 ↓	–	*0.065* ↓	–	0.017 ↓	<0.001 ↓
RAD51AP1	RAD51AP1	–	–	*0.056* ↓	0.023 ↓	*0.059* ↓	<0.001 ↓	*0.079* ↓	0.002 ↓
RAD51C	RAD51C	–	–	0.003 ↓	0.027 ↓	0.024 ↓	0.012 ↓	–	–
RB1	Rb protein	–	*0.054* ↑	0.023 ↑	0.006 ↑	–	0.012 ↑	–	*0.074* ↑
RBBP7	Histone deacet-lase class I	–	–	–	0.019 ↓	–	–	–	0.023 ↓
RBL2	p130	–	–	0.014 ↑	0.018 ↑	–	*0.056* ↑	–	–
RELB	RelB (NF-κB)	0.016 ↑	–	0.032 ↑	–	–	0.048 ↑	0.036 ↑	0.003 ↑
RFC3/4/5	RFC complex	–	–	0.032 ↓	0.016 ↓	–	0.002 ↓	–	*0.054* ↓
SKP2	SKP2	–	–	0.031 ↓	0.019 ↓	0.033 ↓	*0.052* ↓	–	0.002 ↓

Continued

Table 1. *Continued*

Time post-irradiation		5 min		3 h		8 h		24 h	
	Dose (Gy)	0.1	1	0.1	1	0.1	1	0.1	1
SMC4	CAP-C	–	–	–	–	–	*0.052 ↓*	0.006 ↓	<0.001 ↓
SOD2	SOD2	0.018 ↑	*0.091 ↑*	0.009 ↑	0.042 ↑	–	0.025 ↑	*0.079 ↑*	0.017 ↑
STAT3	STAT-3	–	–	0.010 ↑	0.004 ↑	–	0.033 ↑	0.047 ↓	–
STAT5B	STAT-5B	–	*0.082 ↑*	–	–	–	0.002 ↑	–	–
SUMO1	SUMO-1	–	–	–	0.005 ↓	–	–	–	0.007 ↓
TNFRSF1A	TNF-R1	0.021 ↓	0.011 ↓	–	–	–	–	–	–
TNFRSF1B	TNF-R2	<0.001 ↑	0.006 ↑	–	–	–	–	0.002 ↑	0.009 ↑
TNFRSF10B	DR5	–	–	*0.064 ↑*	0.005 ↑	–	0.031 ↑	–	0.006 ↑
TP53BP2	TP53BP2	<0.001 ↑	–	–	0.042 ↑	–	0.003 ↑	–	0.006 ↑
TP53I3	TP53I3	0.038 ↓	–	0.029 ↓	0.003 ↓	–	0.083 ↓	–	–
TP53INP1	TP53INP1	0.017 ↓	–	0.013 ↓	0.038 ↑	–	0.023 ↑	–	–

Genes were considered significant at $P < 0.05$. Genes with *P*-values in ***italic/bold*** font were not included in the pathway analysis for that specific dose-time combination but are included in the tables to demonstrate their pattern of expression if exhibiting modulation at $P < 0.1$. [a]no significant modulation, [b]↑ is upregulation and ↓ is downregulation.

Table 2. Total number of significantly modulated pathways

Time post-IR	5 min			3 h			8 h			24 h		
Dose (Gy)	0.1	1		0.1	1		0.1	1		0.1	1	
	total number		common	total number		common	total number		common	total number		common
DNA damage	0	0	–	1	0	0	5	4	4	1	1	1
Cell cycle	0	0	–	8	2	2	6	13	5	10	10	8
Apoptosis and survival	11	0	–	7	9	2	3	5	2	0	9	0
Immune response	15	0	–	4	7	3	0	6	0	1	4	1
Development	8	0	–	7	10	4	0	7	0	4	20	4
Transcription	2	0	–	3	3	2	0	4	0	0	2	0
Cytoskeleton remodeling	0	0	–	1	1	1	2	0	0	3	2	2
Other	12	0	–	4	6	0	5	6	0	5	8	3
Total	*48*	*0*	*–*	*35*	*38*	*14*	*21*	*45*	*11*	*24*	*56*	*19*

Significantly differentially expressed genes in EpiDermFT exposed to 10 or 1 Gy over a course of 24 h post-IR were placed in functional pathways using MetaCore pathway analysis.

repair and subsequent cell cycle arrest, mainly at the G1/S boundary for 0.1 Gy, and the G2/M boundary for 1 Gy (Table 3). In addition, upregulation of p21 was observed in response to 0.1 and 1 Gy (Table 1), further supporting cell cycle arrest.

As shown in Table 3, ERS1, the SCF complex, and the APC cell cycle pathways were similarly modulated at 3 and 8 h post-IR, indicating that cells were arrested for at least

5 hours. With 0.1 Gy the arrest appeared to be primarily at the G1/S boundary, and at the G2/M boundary with 1 Gy.

At 1 Gy initiation of DNA replication in the early S phase pathway was suppressed (Table 3), as supported by the downregulation of all the hexameric complex subunits (MCM2/3/4/5/6/7) genes (Table 1). These proteins make up the minichromosome maintenance (MCM) complex that is involved in the initiation of DNA synthesis. The pre-

Table 3. Differentially expressed genes that were placed in pathways.

Time post-irradiation	5 min		3 h		8 h		24 h	
Dose (Gy)	**0.1**	**1**	**0.1**	**1**	**0.1**	**1**	**0.1**	**1**
Pathway groups				*P*-values				
DNA damage								
ATM/ATR regulation of G1/S checkpoint	–	–	2.96	NS*	8.61	6.55	–	–
Brca1 as a transcription regulator	–	–	NS	NS	2.87	2.98	–	–
ATM/ATR regulation of G2/M checkpoint	–	–	–	–	4.25	6.38	4.38	3.87
Role of Brca1 and Brca2 in DNA repair	–	–	–	–	4.19	2.98	–	–
Cell cycle								
G1/S: Role of SCF complex in cell cycle regulation	–	–	5.09	3.16	7.28	3.94	NS	3.59
G1/S: ESR1 regulation of G1/S transition	–	–	5.61	5.55	5.42	5.40	NS	3.27
Intra S: Start of DNA replication in early S phase	–	–	–	–	NS	7.65	–	–
Intra S: Transition and termination of DNA replication	–	–	3.28	NS	5.79	6.07	5.28	2.77
G2/M: Role of 14-3-3 proteins in cell cycle regulation	–	–	–	–	NS	3.76	3.69	NS
G2/M: Role of APC in cell cycle regulation	–	–	3.81	NS	2.79	8.80	9.67	12.64
G2/M: Chromosome condensation in prometaphase	–	–	–	–	NS	3.88	9.01	6.86
G2/M: Spindle assembly and chromosome separation	–	–	–	–	2.75	7.49	9.50	6.23
G2/M: The metaphase checkpoint	–	–	–	–	NS	5.06	9.04	13.13
G2/M: Initiation of mitosis	–	–	–	–	NS	4.39	5.64	6.18
Role of Nek in cell cycle regulation	–	–	–	–	–	–	7.13	4.28
Apoptosis and survival								
Anti-apoptotic TNFs/NF-κB/Bcl-2 pathway	4.55	NS	3.91	NS	–	–	–	–
Anti-apoptotic TNFs/NF-κB/IAP pathway	3.87	NS	3.37	NS	–	–	–	–
Apoptosis plus 090609	–	–	NS	3.96	2.87	6.85	NS	3.51
Apoptotic TNF-family pathways	2.79	NS	NS	3.01	–	–	NS	2.70
FAS signaling cascades	3.53	NS	NS	3.71	NS	2.83	NS	3.43
Granzyme B signaling	2.57	NS	2.96	4.69	NS	3.65	NS	2.50
p53-dependent apoptosis	–	–	NS	3.16	2.91	5.92	NS	2.69
Role of IAP-proteins in apoptosis	3.52	NS	5.86	NS	NS	2.90	NS	5.39
TNFR1 signaling pathway	5.32	NS	4.59	2.94	–	–	NS	2.65
Immune response								
Gastrin in inflammatory response	–	–	2.96	3.56	–	–	NS	3.50
IL-1 signaling pathway	2.68	NS	2.92	3.64	NS	2.77	–	–
IL-2 activation and signaling pathway	3.97	NS	NS	3.30	NS	2.50	2.81	3.07
IL-3 activation and signaling pathway	2.64	NS	–	–	NS	2.90	–	–
IL-6 signaling pathway	3.69	NS	3.20	4.06	NS	NS	–	–
IL-7 signaling in T lymphocytes	–	–	NS	2.52	NS	3.17	–	–
IL-22 signaling pathway	2.51	NS	NS	2.85	NS	2.75	–	–
MIF-mediated glucocorticoid regulation	5.57	NS	NS	2.90	–	–	–	–
TLR signaling pathways	2.82	NS	2.95	NS	–	–	–	–

Continued

Table 3. *Continued*

Time post-irradiation	5 min		3 h		8 h		24 h	
Dose (Gy)	0.1	1	0.1	1	0.1	1	0.1	1
Development								
A2B receptor: action via G-protein alpha s	2.39	NS	–	–	–	–	NS	2.31
EGFR signaling via small GTPases	–	–	–	–	–	–	NS	2.50
Endothelin-1/EDNRA signaling	–	–	–	–	–	–	NS	3.61
Gastrin in cell growth and proliferation	2.56	NS	NS	3.95	–	–	NS	2.47
GDNF family signaling	–	–	NS	3.50	–	–	NS	2.49
Glucocorticoid receptor signaling	4.18	NS	NS	3.64	–	–	3.50	3.08
Growth hormone signaling via STATs and PLC/IP3	–	–	–	–	NS	2.61	–	–
HGF signaling pathway	–	–	NS	3.43	–	–	NS	2.45
HGF-dependent inhibition of TGF-beta-induced EMT	4.39	NS	2.96	2.92	NS	4.55	2.90	4.28
IGF-1 receptor signaling	–	–	NS	2.50	–	–	NS	2.96
Regulation of epithelial-to-mesenchymal (EMT) transition	3.15	NS	4.63	NS	NS	2.41	–	–
SSTR1 in regulation of cell proliferation and migration	–	–	–	–	–	–	NS	2.69
TGF-beta receptor signaling	–	–	NS	3.24	–	–	NS	2.31
TGF-beta-dependent induction of EMT via MAPK	2.53	NS	–	–	NS	2.60	–	–
Thrombopoietin-regulated cell processes	–	–	2.86	3.57	NS	4.22	NS	4.13
WNT signaling pathway. Part 1. Degradation of beta-catenin in the absence WNT signaling	–	–	–	–	–	–	2.82	2.48
WNT signaling pathway. Part 2	–	–	5.46	5.39	NS	2.94	5.14	4.41
Transcription								
NF-κB signaling pathway	3.88	NS	2.56	NS	–	–	–	–
Role of AP-1 in regulation of cellular metabolism	3.02	NS	2.56	5.00	NS	3.97	–	–
P53 signaling pathway	–	–	4.07	4.90	NS	4.75	NS	2.87
Role of Akt in hypoxia induced HIF1 activation	–	–	NS	3.34	NS	3.24	–	–
Cell adhesion								
Chemokines and adhesion	2.46	NS	2.87	NS	–	–	2.96	2.89
ECM remodeling	2.31	NS	–	–	–	–	NS	NS
cadherin-mediated cell adhesion	–	–	NS	2.56	–	–	–	–
Integrin-mediated cell adhesion and migration	–	–	–	–	–	–	NS	3.40
Cytoskeleton remodeling								
Cytoskeleton remodeling	–	–	NS	NS	3.05	NS	3.54	4.04
TGF, WNT and cytoskeletal remodeling	NS	NS	4.77	5.34	3.80	NS	5.28	6.40
Others								
CFTR folding and maturation (norm and CF)	–	–	3.95	NS	2.34	NS	–	–
Mucin expression in CF via IL-6, IL-17 signaling pathways	3.29	NS	NS	3.59	NS	2.68	–	–
Mucin expression in CF via TLRs, EGFR signaling pathways	2.35	NS	NS	2.50	–	–	–	–
Muscle contraction: Regulation of eNOS activity in endothelial cells	3.15	NS	2.57	NS	–	–	NS	2.39

Table 3. *Continued*

Time post-irradiation	5 min		3 h		8 h		24 h	
Dose (Gy)	0.1	1	0.1	1	0.1	1	0.1	1
Parkin disorder under Parkinson's disease	3.69	NS	NS	2.54	NS	2.46	–	–
Proteolysis: Putative SUMO-1 pathway	–	–	NS	3.16	–	–	–	–
Proteolysis: Role of Parkin in the Ubiquitin-Proteasomal pathway	3.16	NS	NS	2.72	NS	2.64	NS	NS
Pyruvate metabolism	2.44	NS	2.64	NS	NS	3.92	–	–
Reproduction: GnRH signaling	2.81	NS	NS	3.40	NS	2.65	NS	2.70

Selected pathways significantly modulated in EpiDermFT exposed to 0.1 or 1 Gy. Pathways were considered as significant at false discovery rate (FDR) < 5%. The significant values are presented in the table as the negative log transformation of the *P*-value.

*The modulation of the pathway was calculated as not significant (FDR < 0.05).

NS means not significant, – means that the expression of the gene considered was not significantly changed at the given dose and time.

replication complex (pre-RC), which is activated in the early G1 phase, preparing cells for genomic replication, is composed of MCM, Cdt1, CDC18L, and the origin of replication complex (ORC). TProtein kinase CDC7 and MCM10 that stimulate the recruitment of CDC45L to the pre-RC, Cdt1 and ORC1L were all downregulated, and CDK2 (with an inhibitory effect on CDC18L and MCM4) was upregulated (Table 1). Transition and termination of DNA synthesis was also blocked in tissues irradiated with 1 Gy (Table 3); cyclin-A which is required for inducing DNA replication, the replication factor C (RFC) complex (RFC3/4/5), and the DNA polymerases alpha/primase and epsilon that synthesize DNA were all downregulated (Table 1).

Downregulation of both CDK1 and cyclin-B1 (Table 1) reflected suppression of the initiation of mitosis pathway (Table 3). Activation of the CDK1/cyclin-B complex promotes the progression from G2 to M phase. Upstream regulators (FOXM1, positive transcription regulator of cyclin-B) and downstream effectors of this complex (Lamin-B and KNLS1) were also downregulated (Table 1). CDC20 (Table 1), an activator of the APC whose ubiquitin ligase activity is required to initiate sister-chromatide separation in metaphase, was downregulated.

Only a weak modulation of survival and apoptosis pathways was evidenced in 0.1 Gy (Tables 2 and 3), as indicated by the lack of alteration of key genes in these pathways. By contrast, at 1 Gy, all 5 modulated pathways were proapoptotic, as suggested by the strong upregulation of proapoptosis genes encoding caspase-9, MEKK4, JNK, and c-Jun, and downregulation of cyclin-B1, CDK1, PARP-1, NUMA-1, Lamin-B and survivin (BIRC5) (Table 1).

The large number of genes modulated by 1 Gy compared to 0.1 Gy affected, as expected, the distribution of the number of exclusive genes. Only 113 (~10%) of 1110 radiation-responsive genes detected at 8 h post-IR were exclusive to 0.1 Gy, compared to 815 (~73%) exclusive to 1 Gy (Fig. 1). The 0.1 Gy-exclusive genes fell into 9 significant pathways distributed over a range of cellular processes, whereas the 1 Gy-exclusive genes were represented in over 39 pathways that were strongly associated with cell cycle regulation, DNA damage, and apoptosis (data not shown). Most of the cell cycle pathways were involved in the regulation of G2/M phase transition.

Gene expression 24 h post-IR

The number of radiation-responsive genes 24 h post-IR was similar to that at 8 h, however, with a different distribution between 0.1 and 1 Gy. At 24 h post-IR exclusive genes were ~12% for 0.1 Gy compared to ~27% for 1 Gy. The remaining genes, ~61% common to both doses (Fig. 1), fell into 19 pathways, with a prevalence of cell cycle regulation pathways (Table 2). Overall, at 24 h post-IR, 1 Gy modulated more genes (Fig. 1) resulting in 56 significant pathways being affected compared to only 24 pathways in tissues irradiated with 0.1 Gy (Table 2).

Out of 10 modulated cell cycle regulation pathways, 8 were common to both 0.1 and 1 Gy doses (Table 2). The APC pathway, which targets proteins for degradation to enable chromosome separation and further progression into metaphase, was still greatly affected by both doses. Although none of the APC genes were modulated, genes encoding downstream target proteins such as cyclin-A, cyclin-B, CDK1, and PLK1 with roles in progression through metaphase were downregulated (Table 1).

Collectively, the results suggest that at 24 h post-IR, cells progressed through the S phase and accumulated at G2/M, as supported by the strong modulation of the initiation of the mitosis pathway (Table 3) due to repression of CDC25C and cyclin-B1, cyclin-B2 and CDK1, at both doses (Table 1). Cyclin-B is the obligate activator of

CDK1, and the progression from G2 to M phase is driven by activation of the CDK1/cyclin-B complex; PLK1, which was downregulated, is a key regulator of this complex (Table 1).

The chromosome condensation pathway that ensures all chromosomes are condensed at prometaphase prior to progressing into metaphase was greatly suppressed (Table 3). The condensin complex was downregulated due to repression of CAP-C and CAP-G (Table 1). Both Aurora-A and Aurora-B kinases, which participate in chromosome condensation via phosphorylation of histone H3, were downregulated (Table 1).

The metaphase checkpoint delays chromosome separation at anaphase and the onset of mitotic exit until all chromosomes are connected to the spindle by the kinetochore complex. A kinetochore unattached to the centromer inhibits the activity of CDC20 that activates the APC, which promotes sister-chromatid separation. The metaphase pathway was greatly suppressed by both 0.1 and 1 Gy (Table 3). Genes associated with the various steps of this process were repressed (Fig. 2), ensuring that no chromosome segregation would be carried out.

Proapoptosis pathways were only significantly modulated by 1 Gy (Table 2), of which the role of IAP proteins in apoptosis was the most significant (Table 3). This is indicated by the upregulation of JNK, caspase-9 and Bid, and the downregulation of survivin and HSP70 (Table 1).

Lesser exclusive genes were modulated by 0.1 than by 1 Gy (Fig. 1). The 0.1 Gy-exclusive genes were associated with tissue repair, whereas the 1 Gy-exclusive genes were associated with cell cycle regulation, DNA damage and apoptosis, and the inflammatory response (data not shown). When breaking these processes into pathways, none was significant for 0.1 Gy, while the 12 significant pathways for 1 Gy were distributed between eight proapoptosis and four cell cycle regulation pathways (data not shown).

DISCUSSION

The effects of moderate and high IR doses in humans are well established, while those of LDIR are not. Some studies have shown that cells respond differently to LDIR than to higher IR doses [31, 32], but a consensus on the nature of this response is lacking. Here we sought to
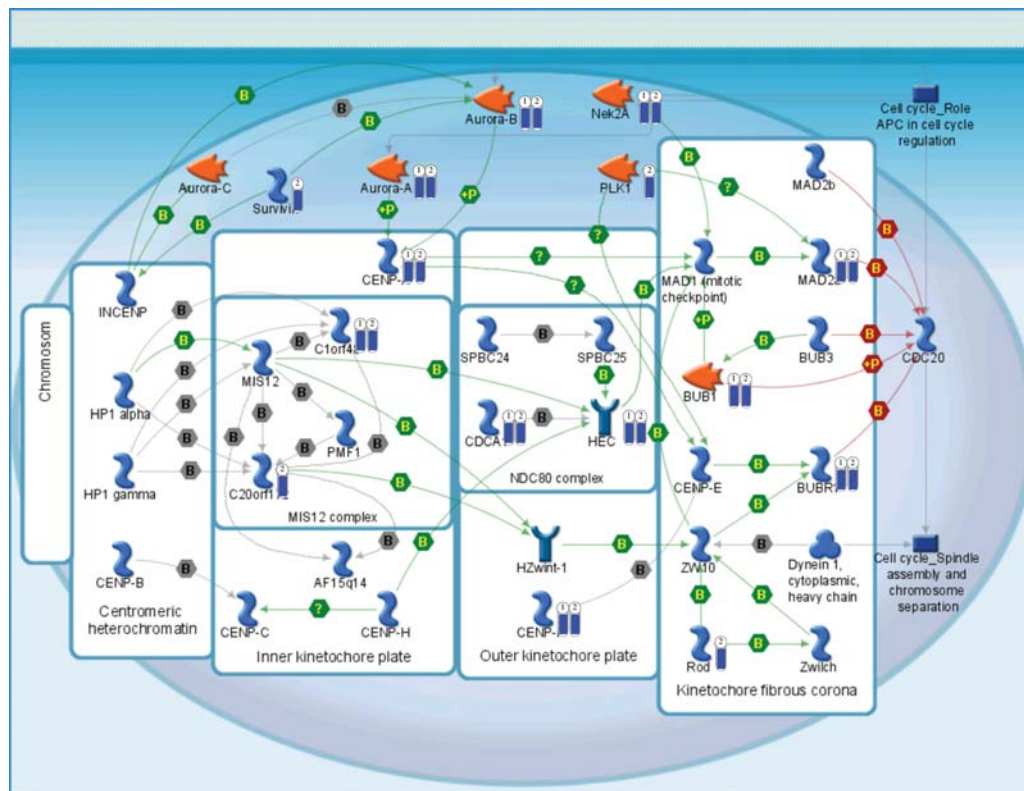

Fig. 2. Illustration of the metaphase checkpoint pathway. Different genes involved in the regulation of the metaphase checkpoint were downregulated in EpiDermFT 24 h after 0.1 or 1 Gy exposure. The color of the bar next to the gene indicates the direction of regulation, where blue is down- and red is upregulation; the circle with the number on top of the bar indicates the group where 1 refers to 0.1 Gy-exposed and 2 refers to 1 Gy-exposed EpiDermFT.

characterize side by side the genomic response to IR following exposure to 0.1 and 1 Gy doses of X-rays. We chose EpiDermFT, a 3D skin model, as our biological system, in order to closely mimic human skin tissue. Furthermore, it is now well established that cells grown in 3D are more radioresistant than their 2D-grown counterparts [9, 10]. EpiDermFT, a reconstruction of the dermal and epidermal skin layers, is thus far the closest *in vitro* model to human skin tissue. This engineered tissue contains two distinct cell types, keratinocytes and fibroblasts, which reproduce the epidermal and dermal skin compartments respectively, and retain *in vivo*-like characteristics; keratinocytes migrate upward away from the dermis and differentiate along the way, while fibroblasts rest at the G1 phase of the cell cycle. Consequently the transcriptional response to IR of EpidermFT represents the sum of the transcriptional responses of keratinocytes and fibroblasts, but is most likely dominated by the actively dividing keratinocytes. While our study is the first to characterize the genomic response in the EpiDermFT system to low versus moderate X-ray doses, another study comparing the transcriptional changes induced by 0.1 and 2.5 Gy proton doses in an epidermis-only 3D skin model (Epi200) has been recently reported [33]. Information regarding cellular processes and functional pathways altered after exposure to low versus moderate IR doses was extracted from global gene expression data. Therefore, presentation and interpretation of data emphasized the pathway placement of significantly modulated genes.

Cellular changes induced by both doses were more time-dependent than dose-dependent, reflecting a response to radiation stress, which is in agreement with other radiation studies [31, 32]. Over the course of 24 h, a total of 5753 dose-responsive genes were detected in EpiDermFT post-exposure to LDIR and MDIR, with MDIR modulating overall more genes than LDIR. Genes modulated by only one IR dose and not the other were defined as unique either to LDIR or MDIR. We found 778 genes unique to LDIR and 1324 genes unique to MDIR. However, these genes do not appear to carry out a unique response for either LDIR or MDIR, but rather exhibit temporal expression specificity, meaning that their modulation by the other dose during another time window, not examined here, is not excluded. Indeed, a considerable number of pathways that were significantly modulated by LDIR and not by MDIR at 3 h post-IR became significant at 8 or 24 h in MDIR-exposed tissues. It was suggested by Ding *et al.* [34] that the modulation of ANLN and KRT15 (cytoskeleton proteins) and GPR51 and GRAP2 (cell–cell signaling) was a unique response to LDIR in primary fibroblasts. By contrast, in our study, only ANLN was modulated, and we observed an earlier and greater suppression of ANLN by MDIR in comparison to LDIR. In agreement with our findings, Jin *et al.* [32] reported that ANLN and KRT15

exhibited a time- but not a dose-response, and that GRAP2 exhibited a complex response in a mesenchymal stem cell line, contradicting the suggestion that these genes are unique to LDIR.

Although 10-fold lower, the 0.1 Gy dose modulated more genes than the 1 Gy dose (752 vs 490, respectively). Exposure of fibroblasts to 0.5 Gy of α particles significantly changed the expression of 709 genes 30 min later [35], but the expression of only 197 genes was altered 4 h post-exposure [36]. Yin *et al.* [31] reported that 0.1, compared to 2 Gy γ-rays, altered a larger number of genes in the brains of mice 30 min after whole body irradiation. Not surprisingly, neither LDIR nor MDIR induced major genes associated with the DNA damage repair pathway immediately after irradiation. The molecular events triggered in the immediate response to IR-induced cellular stress are carried out through post-translational modifications, including phosphorylation, dephosphorylation, and translocation of proteins involved in the DDR response cascade. It is well documented that following detection of DNA damage, the ATM/ATR and Chk1/Chk2 transducers simultaneously phosphorylate two distinct arms of the cell cycle checkpoints [37]. The CDC25 phosphatase arm is rapid, transient, and does not require transcription and accumulation of newly synthesized proteins to carry out cell cycle arrest. The TP53 arm is responsible for the prolonged G1/S cell cycle arrest, and requires the stabilization and accumulation of TP53, which in turn induces the transcription of downstream effectors such as p21. Although direct TP53 modulation was not detected at any of the assessed time-points following either LDIR or MDIR, expression of genes whose transcription is directly regulated by TP53 such as CDKN1A (p21) and MDM2 was altered, indicating that the TP53 DNA damage response was triggered by both LDIR and MDIR in a 5 min to 3 h post-IR time window. In the 3D human epidermis model, network analysis showed that TTP53 dominated the response to 2.5 Gy but not to 0.1 Gy of low LET protons at 4 h and 16 h post-exposure [33].

The largest divergence in response between LDIR and MDIR over the 24 h post-IR time course was exhibited in the first 8 h, and detected, as early as 5 min post-IR. The number of radiation-responsive genes peaked at 3 h, exhibiting about 30% more genes in comparison to the numbers of genes altered at the other time-points. The largest divergence was observed at 8 h post-IR, with 4-fold more genes modulated by HDIR than LDIR.

Taken together, the difference between LDIR and HDIR was in the dynamic of the tissue response. Although the values are the negative Log-transformed *P*-values of the processes and not the fold change, they accurately reflect the kinetics of the various cellular responses to irradiation (Fig. 3). The most pronounced difference was the modulation of genes associated with the DDR cascade. In LDIR,
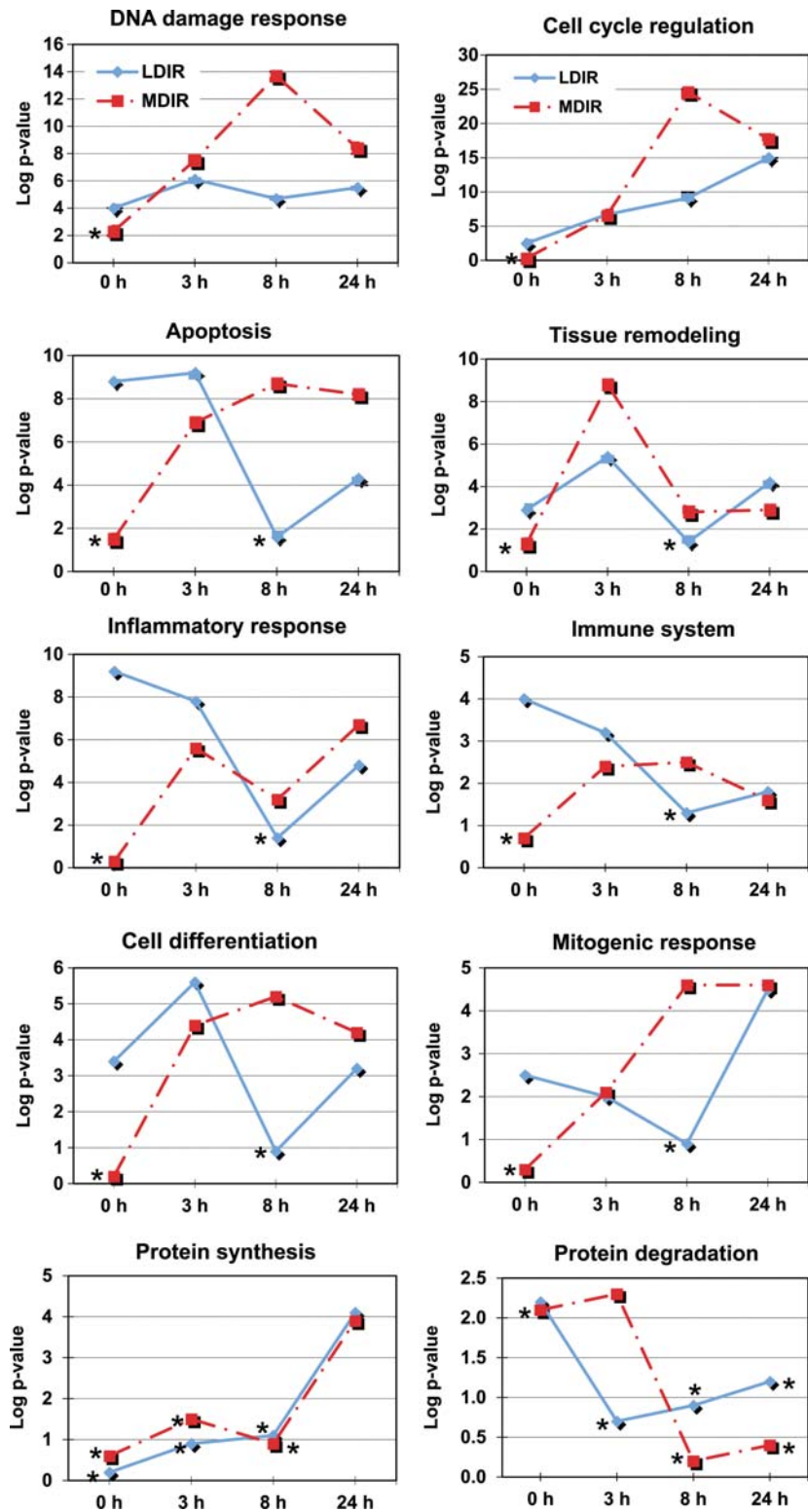
Fig. 3. Representation of the significance level of cellular processes. The most prevalent processes modulated after LDIR and MDIR exposure in EpiDermFT were DNA damage, cell cycle regulation, apoptosis, tissue remodeling, inflammatory and immune response, differentiation and mitogenic response, and protein regulation. Numbers on the *y*-axis are the negative Log-transformation of the *P*-value. *non-significant *P*-value at 5% FDR.

in parallel to a moderate increase of DDR genes over post-IR exposure time, an immediate survival promotion was observed that decreased over time. Irradiation with 0.1 Gy was expected to induce a lower level of DNA damage in EpiDermFT cells than 1 Gy [17]. The initial response to low levels of cellular stress, observed from 5 min to 3 h, was associated with promotion of protection. This is in agreement with observations of protection and repair in brain tissues of mice following 0.1 Gy exposure [30]. As early as 3 h post-LDIR cells attempted cell-cycle re-entry, resulting in an arrest at the G1/S checkpoint beyond 8 h, and followed by an accumulation at the G2/M boundary by 24 h. This long G1/S arrest was accompanied by low transcriptional activity reflected by modulation of only ~200 genes of which 60% were downregulated.

By contrast, the response to HDIR exhibited a more concerted DDR that increased by 8 h and decreased at 24 h post-IR (Fig. 3). In the first hours, cellular mechanisms were geared towards resolving DNA damage, by stalling cell growth, and promoting cell death [37].

Modulation of metaphase regulatory pathways, first detected at 8 h and continued throughout 24 h, supported a prolonged arrest at the G2/M checkpoint. Fibroblasts irradiated with doses ≥1 Gy accumulated in the G2 phase between 6 and 24 h post-IR [38–40]. These observations suggest that by 8 h following exposure to MDIR, cells had repaired most, but not all, of their damaged DNA. The remaining DNA damage, similar in magnitude to that inflicted by LDIR, induced cell–cell signaling events similar to those observed in the early response to LDIR, resulting in the promotion of cell growth. DNA damage in 3D skin models irradiated with 1 Gy was above background levels at 8 h post-IR, and returned to background levels 12–24 h post-exposure [17, 40].

Although at 24 h MDIR modulated more genes and diverse pathways than LDIR, the modulated cellular processes were very comparable for both doses. Predominant processes were cell cycle regulation, followed by DNA damage, apoptosis and inflammatory response. In a mesenchymal stem cell line, the late response phase (12 and 48 h post γ-irradiation) showed no differential gene expression between the low (0.01, 0.05, and 0.2 Gy combined) and moderate (1 Gy) doses [26]. In the 3D human epidermis model, the peak of genes with altered expression in response to 2.5 Gy coincided with the 24 h post-exposure time-point, while that in response to 0.1 Gy occurred at 16 h post-IR [33]. In ex vivo irradiated human skin, differentially-expressed genes peaked at 30 h post exposure for both X-ray doses tested, 0.05 and 5 Gy [41]. Besides the model itself, differences in gene expression from a quantitative perspective for different skin models in response to low and moderate IR doses can be attributed to differences in the types of IR used, as well as the way the data analyses were conducted.

Although we did not assess gene expression later than 24 h post-IR, it is clear from the data that the response to the insult was still ongoing and similar in magnitude for both LDIR and MDIR, since cells in both groups appeared to be arrested at the G2/M checkpoint.

CONCLUSION

In summary, our gene expression results support the growing evidence for non-linearity of the response to low versus high IR doses. Put simply, it seems that an acute exposure to LDIR promotes tissue protection and survival as an initial response to the stress, to allow 'assessment' of the challenge intensity in order to mount an appropriate response. MDIR on the other hand, promotes apoptosis to eliminate cells with considerable DNA and other cellular damage, followed by a response promoting growth and survival. The evolution of the transcriptional response over 24 h in EpidermFT exposed to 0.1 Gy is overall consistent with the conclusion from studies conducted by our laboratory on skin exposed in vivo to 0.1 Gy and ex vivo to 0.05 Gy: in response to low-dose radiation, human skin initiates a transcriptional program to enhance survival [41–43].

FUNDING

ACKNOWLEDGEMENTS

REFERENCES

1. Redpath JL. Radiation-induced neoplastic transformation in vitro: evidence for a protective effect at low doses of low LET radiation. *Cancer Metastasis Rev* 2004;**23**:333–9.
2. Preston DL, Pierce DA, Shimizu Y *et al*. Dose response and temporal patterns of radiation associated solid cancer risks. *Health Phys* 2003;**85**:43–6.
3. Preston RJ. The LNT model is the best we can do–today. *J Radiol Prot* 2003;**23**:263–8.
4. Brenner DJ, Doll R, Goodhead DT *et al*. Cancer risks attributable to low doses of ionizing radiation: Assessing what we really know. *Proc Natl Acad Sci USA* 2003;**100**:13761–6.
5. NRC (National Research Council). 2006. *Health Risks from Exposure to Low Levels of Ionizing Radiation*. BEIR VII Phase 2. Washington, DC: National Academy Press.

Available from: http://www.nap.edu/openbook.php?record_id=11340&page=1

6. Royal HD. Effects of low level radiation-what's new? *Semin Nucl Med* 2008;**38**:392–402.

7. Prise KM. New advances in radiation biology. *Occup Med* 2006;**56**:156–61.

8. Karagiannis TC, El-Osta A. Double-strand breaks: signaling pathways and repair mechanisms. *Cell Mol Life Sci* 2006;**61**:2137–47.

9. Sowa MB, Chrisler WB, Zens KD *et al*. Three-dimensional culture conditions lead to decreased radiation induced cytotoxicity in human mammary epithelial cells. *Mutat Res* 2006;**687**:78–83.

10. Storch K, Eke I, Borgmann K *et al*. Three-dimensional cell growth confers radioresistance by chromatin density modification. *Cancer Res* 2010;**70**:3925–34.

11. Hayden PJ, Stolper G, Cooney C *et al*. Healing of dermal wounds in the EpiDerm-FT™ in vitro human skin model: An animal alternative for wound healing issues. *The Toxicologist* 2008;**102**:69.

12. Moore JO, Stebbins WG, Guevara D *et al*. Human skin equivalent: A reliable in vitro model for carcinogenic experiments. *J Invest Dermatol* 2004;**122**:A23.

13. Moore JO, Wang Y, Stebbins WG *et al*. Photoprotective effect of isoflavone genistein on ultraviolet B-induced pyrimidine dimer formation and PCNA expression in human reconstituted skin and its implications in dermatology and prevention of cutaneous carcinogenesis. *Carcinogenesis* 2006;**27**:1627–35.

14. Afaq F, Zaid MA, Khan N *et al*. Protective effects of pomegranate-derived products on UVB mediated damage in human reconstituted skin. *Exp Dermatol* 2009;**18**:553–61.

15. Flockhart RJ, Diffey BL, Farr PM *et al*. NFAT regulates induction of COX-2 and apoptosis of keratinocytes in response to ultraviolet radiation exposure. *FASEB J* 2008;**22**:4218–27.

16. Murray AR, Kisin E, Leonar SS *et al*. Oxidative stress and inflammatory response in dermal toxicity of single-walled carbon nanotubes. *Toxicology* 2009;**257**:161–71.

17. Su Y, Meador JA, Geard CR *et al*. Analysis of ionizing radiation-induced DNA damage and repair in three-dimensional human skin model system. *Exp Dermatol* 2010;**19**:e16–e22.

18. Hei TK, Ballas LK, Brenner DJ *et al*. Advances in radiobiological studies using a microbeam. *J Radiat Res* 2009;**50** Suppl A:A7–12.

19. Schmid TE, Dollinger G, Hable V *et al*. Relative biological effectiveness of pulsed and continuous 20 MeV protons for micronucleus induction in 3D human reconstructed skin tissue. *Radiother Oncol* 2010;**95**:66–72.

20. Miller JH, Suleiman A, Chrisler WB *et al*. Simulation of electron-beam irradiation of skin tissue model. *Radiat Res* 2011;**175**:113–8.

21. Belyakov OV, Mitchell SA, Parikh D *et al*. Biological effects in unirradiated human tissue induced by radiation damage up to 1 mm away. *Proc Natl Acad Sci USA* 2005;**102**:14203–8.

22. Sedelnikova OA, Nakamura A, Kovalchuk O *et al*. DNA double-strand breaks form in bystander cells after microbeam irradiation of three-dimensional human tissue models. *Cancer Res* 2007;**67**:4295–302.

23. Curren RD, Mun GC, Gibson DP *et al*. Development of a method for assessing micronucleus induction in a 3D human skin model (EpiDerm). *Mutat Res* 2006;**607**:192–204.

24. Netzlaff F, Lehr CM, Wertz PW *et al*. The human epidermis models EpiSkin, SkinEthic and EpiDerm: an evaluation of morphology and their suitability for testing phototoxicity, irritancy, corrosivity, and substance transport. *Eur J Pharm Biopharm* 2005;**60**:167–78.

25. Rocke DM, Durbin BP. A model for measurement errors for gene expression arrays. *J Comp Biol* 2001;**8**:557–69.

26. Durbin BP, Hardin J, Hawkins D *et al*. A variance-stabilizing transformation for gene expression microarray data. *Bioinformatics* 2002;**18**:S105–10.

27. Durbin BP, Rocke DM. Estimation of transformation parameters for microarray data. *Bioinformatics* 2003;**19**:1360–7.

28. Rocke DM, Durbin BP. Approximate variance-stabilizing transformation parameters for microarray data. *Bioinformatics* 2003;**19**:966–72.

29. Rocke DM. Design and analysis of experiments with high throughput biological assay data. *Semin Cell Dev Biol* 2004;**15**:703–13.

30. Benjamini Y, Hochberg Y. Controlling the false discovery rate: a practical and powerful approach to multiple testing. *J R Stat Soc, Series B* 1995;**57**: 289–300.

31. Yin E, Nelson DO, Coleman MA *et al*. Gene expression changes in mouse brain after exposure to low-dose ionizing radiation. *Int J Rad Biol* 2003;**79**:759–75.

32. JJin YW, Na YJ, Lee YJ *et al*. Comprehensive analysis of time- and dose-dependent patterns of gene expression in a human mesenchymal stem cell line exposed to low dose ionizing radiation. *Oncol Rep* 2008;**19**:135–44.

33. Mezentsev A, Amundson SA. Global gene expression responses to low- or high-dose radiation in a human three-dimensional tissue model. *Radiat Res* 2011;**175**:677–88.

34. Ding LH, Shingyoji M, Chen F *et al*. Gene expression profiles of normal human fibroblasts after exposure to ionizing radiation: a comparative study of low and high doses. *Radiat Res* 2005;**164**:17–26.

35. Ghandhi SA, Ming L, Ivanov VN *et al*. Regulation of early signaling and gene expression in the alpha-particle and bystander response of IMR-90 human fibroblasts. *BMC Med Genomics* 2010;**3**:31.

36. Ghandhi SA, Yaghoubian B, Amundson SA. Global gene expression analyses of bystander and alpha particle irradiated normal human lung fibroblasts: synchronous and differential responses. *BMC Med Genomics* 2008;**1**:63.

37. Lukas J, Lukas C, Bartek J. Mammalian cell cycle checkpoints: signalling pathways and their organization in space and time. *DNA Repair* 2004;**3**:997–1007.

38. Zhou T, Chou JW, Simpson DA *et al*. Profiles of global gene expression in ionizing radiation-damaged human diploid fibroblasts reveal synchronization behind the G1 checkpoint in a G0-like state of quiescence. *Environ Health Perspect* 2006;**114**:553–9.

39. Kim CS, Kim JK, Nam SY *et al*. Low-dose radiation stimulates the proliferation of normal human lung fibroblasts via a transient activation of Raf and Akt. *Mol Cells* 2007; **24**:424–30.

40. Suzuki K, Nakashima M, Yamashita S. Dynamics of ionizing radiation-induced DNA damage response in reconstituted three-dimensional human skin tissue. *Radiat Res* 2010;**174**:415–23.

41. Albrecht H, Durbin-Johnson B, Yunis R *et al*. Transcriptional response of ex vivo human skin to ionizing radiation: comparison between low- and high-dose effects. *Radiat Res* 2012;**177**:69–83.

42. Goldberg Z, Rocke DM, Schwietert C *et al*. Human in vivo dose-response to controlled, low dose low linear energy transfer ionizing radiation exposure. *Clin Cancer Res* 2006;**12**: 3723–9.

43. Berglund SR, Rocke DM, Dai J *et al*. Transient genome-wide transcriptional response to low-dose ionizing radiation in vivo in humans. *Int J Radiat Oncol Biol Phys* 2008;**70**:229–34.